Dynamic Optical Tweezers using Acousto-Optic Modulators

Author: Júlia Ferrer Ortas
Facultat de Física, Universitat de Barcelona, Avinguda Diagonal 645, 08028 Barcelona, Spain.

Advisors: Estela Martín Badosa and Mario Montes Usategui

Abstract: This work consists of the study, characterisation and set-up of an Acousto-Optic Light Modulator made up of two TeO_2 crystals, to use it in an optical tweezers system. We have performed the following tasks: optical system assembly and alignment, optimization of the first diffraction order efficiency of the device and, finally, deflection analysis. Furthermore, we have developed a control system based on a multi-function data acquisition board and a software using LabVIEW that allows the user to dynamically control the position of the laser spot, as well as its amplitude. Lastly, we have improved the program making possible the use of time-sharing trapping.

I. INTRODUCTION

Optical Tweezers are instruments that consist of a light beam that is highly focused by an objective with a high numerical aperture [1]. Light is capable of accelerating and trapping microscopic particles -ranging between hundreds of nanometers and a few micrometers- near the focus of the beam, which is known as optical trap.

The most basic tweezers system uses one laser beam, allowing the generation of a single trap. By diverting the incident beam we can change its position, therefore, we can move and manipulate the trapped particle. In more complex experiments, however, we can be interested in having more than one trap simultaneously, either to trap several particles at the same time or to manipulate larger structures (common in biological processes).

Two permanent optical traps can be created using a beam-splitter. It divides the original beam into two of them, which can be handled separately to produce two different trapping sites. However, if we want to move the trap in a dynamic way or generate multiple traps it is convenient to use alternative, more flexible approaches. There are two main technologies for this purpose: using a diffractive element such as liquid crystal spatial light modulators (LC-SLMs) or by time-multiplexing, in which the laser is scanned between different positions using acousto-optic deflectors (AODs).

Liquid crystal displays are able to spatially modify the properties of incoming wavefronts, allowing tilting or defocusing the beam to change the position of the trap in 3D. They can also generate arbitrary patterns of traps, by using the principles of digital holography [2]. They have the advantage that the traps are permanent, but the main drawback is that the holograms can only be updated at around 60 Hz.

Acousto-optic modulators, on the other hand, only allow a controlled deflection of the beam in 2D, meaning that at a given time there is only one active trap located at a designated spatial position. Since AODs deflect light at a very high rate (up to around 100 kHz), multiple traps can be generated by time-sharing [3]. This means that the laser visits different positions such that each trap is refreshed at times much smaller than the diffusion time of the trapped particle to prevent it from drifting away, while the laser switches to another position. In other words, the laser visits each trap so frequently that the particle does not notice it has moved. The traps are not permanent in time, but this is unimportant to many applications.

In the *Biopt* group from the *Departament de Física Aplicada i Òptica* they have an holographic optical tweezers system, using a LC-SLM. The goal of this project is to set-up an optical trapping system with an AOD (Fig.1) to use the time-sharing operating mode.

Acousto-Optic Deflectors

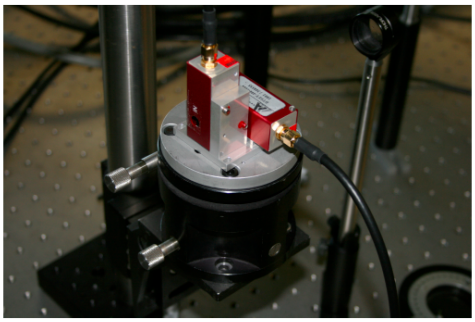

FIG. 1: Picture of our modulators.

When an acoustic wave travels through an acousto-optic material it generates variations in its refractive index that result in a phase grating along the crystal. We can control the periodicity of the grating by changing the frequency of a radiofrequency electrical signal (RF) transduced to the crystal with a piezoelectric element, and treat it as a diffraction grating. Hence, a set of parallel reflectors separated by the wavelength of sound Λ will reflect light if the incident angle θ satisfies the Bragg condition for constructive interference of the first diffraction order,

$$\sin\theta_B = \frac{\lambda}{2\Lambda}, \tag{1}$$

where λ is the wavelength of the incident light ($\lambda = 1064$ nm in our case). Equation (1) (assuming θ_B to be small) leads us to

$$\theta_B = \sin^{-1}\frac{\lambda}{2\Lambda} = \sin^{-1}\frac{F\lambda}{2v_s} \approx \frac{\lambda}{2v_s}F, \qquad (2)$$

where F and v_s are the frequency and the velocity of the acoustic wave, respectively [4]. Given the wavelength of our laser and that v_s depends on the material (650 m/s for TeO_2), each Bragg angle will have its corresponding acoustic frequency. Our crystal is cut at a fixed angle that corresponds to the frequency F_0. For an angle of incidence θ the first diffraction order is diverted 2θ from the non-diffracted beam (zero order), as shown in Fig.2. To achieve modulation we can apply a frequency $F = F_0 \pm \Delta F$ that will result in a deflection for the first order of $2\theta_B \pm \Delta\theta$, where

$$\Delta\theta = \frac{\lambda}{v_s}\Delta F. \qquad (3)$$

When following Bragg condition, there is a tolerance that defines a range of frequencies around F_0, known as the central frequency, in which diffraction happens successfully. This is called the deflector bandwidth (in our case 30 MHz) and determines the maximum angle of deflection that we can obtain.

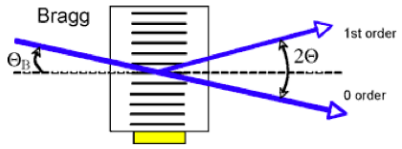

FIG. 2: Geometrical explanation of 2θ deflection of the first diffraction order [5].

Using the combination of two perpendicular crystals it is possible to move the laser beam two-dimensionally. The intensity of the diffracted beam can also be modulated by varying the amplitude of the acoustic wave by means of the RF power.

II. SET-UP AND EFFICIENCY MEASUREMENTS

The first task we have done is setting up the optical system. The acousto-optic device has been placed in a micrometric mechanical platform that allows its accurate movement, as efficiency highly depends on its orientation and position. Then, we have proceeded with the identification of the 1-1 order (first order in both axis), which is the one to be optimized. We have aligned the system and adjusted the three degrees of freedom of the platform, as well as its horizontal and vertical positions, so that the efficiency is optimal. Lastly, we have also optimized the convergence of the incident beam.

Our procedure has been the following: with a power meter (Thorlabs S130A) we have measured the power before the AOD and after it, at a determined distance. The efficiency is the ratio between the power measured after the AOD and the power measured before it.

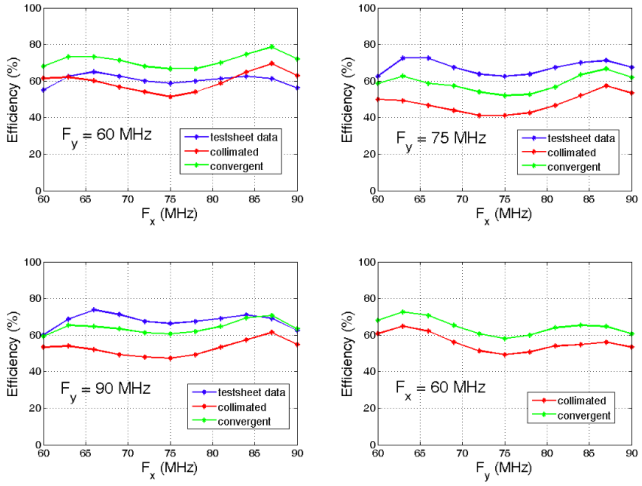

FIG. 3: Efficiency measurements in different cases in which the frequency of one axis is fixed while the other is swept through the bandwidth, compared to the testsheet data.

The results are shown in Fig.3 (typical efficiency error: $\delta_{Eff} = 2\%$.). We present two experimental curves corresponding to a collimated beam and a convergent beam, as well as the data from the testsheet provided by the manufacturers. We have studied several cases corresponding to a fixed frequency for one axis and a sweep through the whole bandwidth for the other. As we can see, we have reproduced the efficiency curves given in the testsheet and even achieved better values. Also, the efficiency is higher if the beam is slightly convergent than if it is collimated.

We have also analysed the effect of the RF power - or, equivalently, the amplitude of the acoustic wave- on the efficiency. We already knew that it grows with the RF power, but the manufacturer advised us that at some point it could diminish, for very high RF powers, so we want to be sure that we are working at the optimal power value. We have measured it at different points (for both F_x and F_y fixed) and in all cases we have obtained similar curves. In Fig.4 we present one of them as an example.

We have studied three different cases, in two of them we changed the power of one axis while the other was set to the maximum and in the third one they changed together.

From the results, we have decided to work from now on with a RF power of around 1.1 W, which ensures the maximum efficiency.

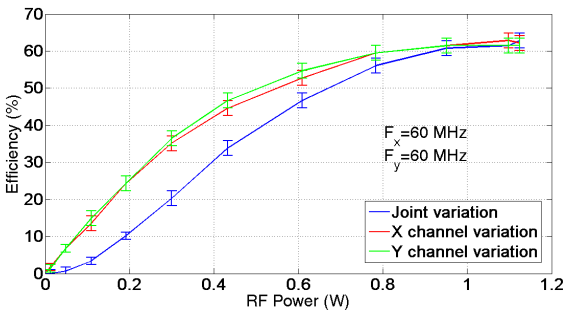

FIG. 4: Dependence of the efficiency with the RF power on the point $F_x = F_y = 60$ MHz.

III. DEFLECTION MEASUREMENTS

Next we have studied deflection properties. The first step has consisted of setting up all the elements of the optical tweezers system. The original beam leaves the laser with a nominal size of 5.2 mm and linearly polarized in the horizontal direction. Our first element is a half-wave plate ($\lambda/2$) at 45º from the horizontal axis to rotate the polarization 90º, because the AOD requires an input beam having a vertical, linear polarization. It has been unnecessary in our set-up to expand the beam size because, according to the specifications of the device given by the manufacturers, the input beam on the AOD needs to be between 1.2 and 6.0 mm to have an optimal efficiency. As our beam is 5.2 mm in size, we have decided not to add any additional optics before the AOD, to make the set-up as simple as possible.

After the half-wave plate the beam enters the pair of acousto-optic X and Y deflectors, and at the exit we have built a telescope to magnify the beam size from 5.2 to 8 mm, in order to adapt it to the aperture of the microscope objective.

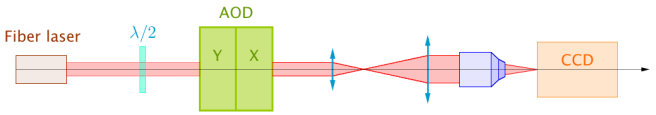

FIG. 5: Diagram of the experimental system. For our convenience, in the experiments we have replaced the microscope objective by a 100 mm focal length lens.

With the lens available in the lab, we have chosen two of them giving the right magnification and with the highest focal lengths, to avoid aberrations as much as possible. We have used an objective and an ocular of $f'_1 = 125$ mm and $f'_2 = 200$ mm of focal length, respectively. With this information we can work out the size of the resulting beam using paraxial optics laws:

$$\frac{y'}{y} = \frac{f'_2}{f'_1} \; ; \; \frac{y'}{5.2} = \frac{200}{125} \rightarrow \; y' = 8.32 \text{ mm}. \qquad (4)$$

In this way, the beam slightly overfills the microscope objective, as is commonly done in optical tweezers set-ups.

Finally, as shown in Fig.5, the beam is focused at the image focal plane of the microscope objective, where the optical trap is formed. We have placed a CCD camera (Imagingsource, DMK 22BUC03) sensitive to infrared radiation in order to see and monitor the movement of the laser spot (1-1 order).

Now we are ready to study deflections. First of all we have taken several images with the camera for different positions of the spot. In particular, we have fixed the frequency of one axis and swept the other through the bandwidth in steps of 3 MHz (one image for each step). By repeating the process for both axis we have obtained vertical and horizontal trajectories. Sweeping both axis at the same time we have also got a diagonal trajectory.

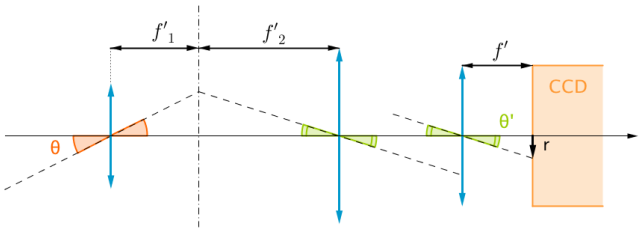

FIG. 6: Ray tracing for our system.

After that, we have analysed the images with an image processing program that allows us determining the position in pixels of each spot. Knowing the pixel dimensions (6x6 μm^2) we can calculate the relative position (r) of all the spots taking the central position ($F_x = F_y = F_0 = 75$ MHz) as a reference: $r^2 = (x - x_0)^2 + (y - y_0)^2$, where x, y are the coordinates of the point under study and x_0, y_0 the coordinates of the reference.

We are interested in the angles of deflection measured from the optical axis. The distance between the "screen" (CCD sensor) and the focusing lens is its focal length: $f' = 100$ mm. Considering that the system has revolution symmetry for all the measured radial coordinates (r) we can work out an angle, defined as follows (Fig.6):

$$\theta' = \tan^{-1} \frac{r}{f'}. \qquad (5)$$

Taking into account the magnifying system, the deflection angles just after the AOD are:

$$\theta = \theta' \cdot \frac{f'_2}{f'_1} = \left[\tan^{-1} \frac{r}{f'}\right] \cdot \frac{f'_2}{f'_1}. \qquad (6)$$

We find that the maximum angle of deflection (for the spot on one end of the diagonal trajectory) is $\theta \approx (1.99 \pm 0.03)°$. Therefore we confirm that the hypothesis of small angles is correct.

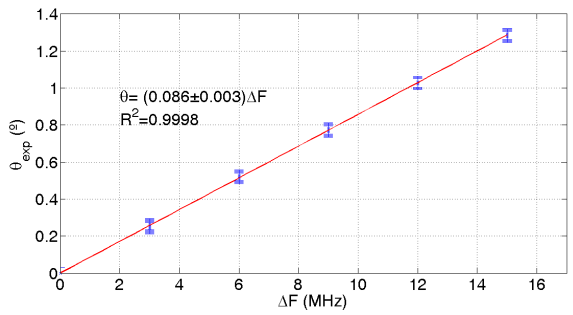

FIG. 7: Experimental angles against frequency.

To continue with the study we can now compare our results with the theory. In Fig.7 we present the experimental angles against frequency and the correspondent linear regression (the independent term is around 10^{-5} and, therefore, negligible). The dependence is remarkably linear as shown by the regression coefficient ($R^2 \approx 0.9998$).

Following equation (3) we can check if the theoretical and experimental slopes match. With the nominal values taken from the testsheet we find that:

$$\frac{\lambda}{v_s} = \frac{1064 \cdot 10^{-9}\ \text{m}}{650\ \text{m/s}} \cdot \frac{180^\circ \cdot 10^6\ \text{Hz}}{\pi\ \text{rad} \cdot 1\ \text{MHz}} \approx 0.094\ ^\circ/\text{MHz} \quad (7)$$

It is essentially the same value as ours (0.086 ± 0.003 $^\circ$/MHz), taking into account that we can have small errors in the magnification of our system, due to the beam being slightly convergent.

IV. CONTROL SYSTEM DEVELOPMENT

This second part of the project is highly experimental as well, although it is focused on electronics and software. Connected to the AODs, we have a device called DDSPA (Direct Digital Synthesizer + Amplifier) that generates and sends the RF signals to the piezoelectric transducer. Apart from that, a control system connects to the DDSPA and receives instructions from the users PC. The manufacturers have provided a control interface through an USB 2.0 link to do it, surprisingly, data are sent by means of a connection that limits the updating rate to hundreds of Hz, while the technology allows rates of several hundreds of kHz. Moreover, with the software provided by the manufacturers the user cannot dynamically vary the values of the variables -frequency and power of the RF- since any change requires him or her to type the new values and to press a button for updating them, which is not useful for the research.

For this reason, we have performed two tasks: we have replaced the USB controller by a PCI-6229, a multifunction data acquisition board from National Instruments (NI-DAQ) installed on the computer, with two Connector Blocks connected to the DDSPA, and we have also developed a suitable software in LabVIEW code. It allows dynamic variation of the parameters, to arbitrarily position one trap in two-dimensions, and also to implement the time-sharing operation mode for the creation of more than one trap.

The two Connector Blocks of the PCI-6229 have 68 screw terminals each. We have used 26 of them for each channel (X and Y) wiring 26 pins of a DB44HD, a 44-pin cable, which connects to the DDSPA at the other end.

It is relatively easy to communicate with the board using a software developed in LabVIEW code, explained next, because the programming language includes all specific functions for it. The PCI-6229 board is capable of several functions among analog or digital, input or output, counters, etc. Our software consists of 24 digital outputs for each channel arranged as follows. 8 bits are assigned to the amplitude, which consequently can be ranged from 0 to 255. Frequency is encoded in a 15-bit variable defined by the manufacturers as

$$N = \frac{F(\text{MHz}) \cdot 2^{15}}{500}. \quad (8)$$

That means that if we want to send, for example, the central frequency ($F_0 = 75$ MHz): $N = 4915.2$. To send it we first have to round it to an integer and then write it in binary code. Thus, what we send is the pattern 001001100110011.
There is an extra bit left, which is used for security to lock all other bits if needed. Each channel also requires two common grounds taken as a reference.

When sending information to the board a hierarquically organised sequence must be followed: creating, starting and writing data in a LabVIEW DAQ task, and then stopping and clearing it. Through this succession we determine the type of task (digital output, as said before) as well as the physical terminals of the Connector Block ports that we are setting up.

We have first focused on achieving single trap dynamic control. The information is written in the task using the LabVIEW "DAQ Write" function. The advantage of our software compared to the provided one is hidden in this function. We can set it inside a while loop together with the variable control, so that when the user changes the value it works immediately because it is continuously writing. The while loop condition is wired to a stop button that the user presses when he or she wants to stop the execution. When it happens, the data flow leaves the loop and the task line continues to complete the process. Before sending the signals to the DDSPA for the AOD control, we have verified them by means of an oscilloscope. We have then successfully tested the program in the experimental set-up, allowing us to drive the spot to any position within the F_x-F_y plane.

At this point our aim was improving the software to allow time-sharing operation mode at 100 kHz rate. The idea is that the user defines n positions on the frequency

plane (set as elements of a column array) where he or she wants the multiple spots to be. The program must include periodic conditions meaning that after the last element it comes the first position again.

However, the most crucial point here is timing. As the final aim is to trap several particles simultaneously, timing has to be very precise, otherwise the trap could not be effective and particles could escape.

We first tried a timing control based on software using a timed loop, but it is unreliable as Windows is not a real-time operative system. Consequently, to get shorter and more precise periods it has been necessary the use of hardware timing, available in the PCI-6229 board. It can provide a time base of 100 kHz, which is precisely what we need. This can be handled using the LabVIEW "DAQ timing" function within the task line. In short, in this second step of the software development we have only changed the part of the code related to frequency, while the other variables -amplitude and security lock- keep working as explained in the first part. Before running the program, we have taken preventive measures and ensured that all structures of the code are well synchronized.

With this new software development, we have been able to deal with several traps at the same time with a regular frequency signal. This has allowed us to satisfactorily generate multiple traps in an optical tweezers system by time-sharing (Fig.8).

V. CONCLUSIONS

The results we have obtained are proof of concept. Now that the new control system and software are ready, efficiency and deflection measurements could be repeated in a more automatic way. Regarding efficiency, the set-up could be adapted so that the final beam reached the power meter sensor for any position on the $F_x - F_y$ plane. In that way we could easily take a greater amount of images without any movements of the power meter to have more points characterised, instead of moving the sensor position for every image as we had to do.

In addition, as we have checked that the efficiency is not constant through the bandwidth, the software could include the suitable correction factor to adjust the efficiency in each position to make traps always equally bright. This is critical for the proper functioning of the trap, otherwise the forces applied to the trapped particle would vary with the position.

Moreover, with a more capable PCI board it is possible to use a 31-bit frequency variable with the DDSPA (instead of our version of 15 bits). This would enhance the resolution of the system. With our current version, the minimum deflection angle that we can get is $\theta \approx 1.43 \cdot 10^{-3^\circ}$, but with the mentioned improvement, we could obtain a resolution of $\theta \approx 2.19 \cdot 10^{-8^\circ}$, which would allow more accurate manipulations.

The front panel of the software could also be modified to make things easier to the user converting it into an executable file.

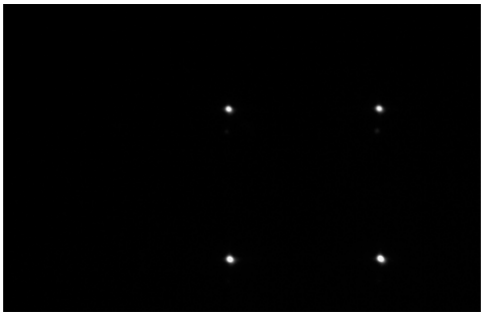

FIG. 8: Image taken in the lab of 4 laser spots obtained with time-sharing operating mode.

Acknowledgments

First of all I want to thank my advisors Estela Martín Badosa and Mario Montes Usategui for having entrusted me this project. We have invested many hours doing experimental tasks such as optical alignment and there have been some experimental problems to solve. The control system development has been also laborious and they have always been patient with me.

To conclude, I would like to thank my friends, because they are always there to help and also my parents and my family because without them I would not be here.

[1] A. Ashkin, "Acceleration and trapping of particles by radiation pressure", Phys. Rev. Lett. 24, 156–159 (1970).

[2] J. E. Curtis, B. A. Koss, D. G. Grier, "Dynamic holographic optical tweezers", Opt. Commun. 207, 169-175 (2002).

[3] W. H. Guilford, J. A. Tournas, D. Dascalu, D. S. Watsona, "Creating multiple time-shared laser traps with simultaneous displacement detection using digital signal processing hardware", Anal. Biochem. 326, 153–166 (2004).

[4] M. Schwingel (2012), *Multiple trap optical tweezers for cell force measurements* (PhD Thesis), Karlsruher Instituts für Technologie (KIT) - Universitätsbereich genehmigte.

[5] AA Opto Electronic, *Acousto-optic Theory Application Notes* http://www.aaoptoelectronic.com/Documents/AAOPTO-Theory2013-4.p

[6] National Instruments, *M Series User Manual*, http://digital.ni.com/manuals.nsf/websearch/2025C99AB0614F9E8625748000577B9A